Sulfur Isotope Studies in Solid Organics: A Protocol for Utilizing Heterogeneous Standards and Secondary Ion Mass Spectrometry

ARTICLE *in* ENERGY & FUELS · APRIL 2014

Impact Factor: 2.79 · DOI: 10.1021/ef5001776

5 AUTHORS, INCLUDING:

Mindy M. Zimmer
Pacific Northwest National Laboratory
23 PUBLICATIONS **342** CITATIONS
SEE PROFILE

Firdaus Janoos
The Ohio State University
11 PUBLICATIONS **28** CITATIONS
SEE PROFILE

energy&fuels

Article

pubs.acs.org/EF

Sulfur Isotope Studies in Solid Organics: A Protocol for Utilizing Heterogeneous Standards and Secondary Ion Mass Spectrometry

Hubert E. King, Jr.,* Mindy M. Zimmer,† William C. Horn, William A. Lamberti, and Firdaus Janoos

Corporate Strategic Research, ExxonMobil Research and Engineering Co., Annandale, New Jersey 08801, United States

Supporting Information

ABSTRACT: We present sulfur isotope compositions ($^{34}S/^{32}S$) for nine solid organics—six petroleum cokes and three solid bitumens—demonstrating a reliable method using secondary ion mass spectrometry (SIMS) for complex, inhomogeneous materials. The protocol uses a homogeneous working standard, a heterogeneous matrix standard, and statistical measures to identify outliers in the analyses. We demonstrate screening methods that minimize the impact of heterogeneities on the SIMS data, leading to a calibrated matrix correction that can facilitate analysis of sulfur isotope composition in solid organics. The thiophenic sulfur and low H/C matrices of the selected materials are good surrogates for many solid organics. Furthermore, the approach is generally applicable to a wide range of materials and provides a means to obtain meaningful SIMS data when suitable homogeneous standards are unavailable.

1. INTRODUCTION

For several decades, the importance of sulfur isotope analysis in understanding petroleum origin and evolution has been recognized.[1−3] In particular, Krouse[2] discussed the several possible effects that lead to changes in sulfur isotope ratios and how these can be related to oil and gas generation. Since those early studies, it has become commonplace for those in industry and academia to study the sulfur isotopes of H_2S gas, petroleum liquids, and associated sulfide minerals.[3−7] Analysis of the solid organic fraction is less common.[8−10] Organic solids are not always available as homogeneous samples. Their formation conditions can lead to intermixed sulfates or sulfides, making the interpretation of results by conventional bulk isotopic analysis problematic. In addition, solid bitumen, as formed in nature, is often found as small, intergrain accretions, grain coatings or inclusions, requiring microanalysis, where small (spatially) contaminants can be an issue. Secondary ion mass spectrometry (SIMS) has been used but the needed accuracy to address many geologic issues has been hampered because of an inadequate matrix correction for solid organics.

Our search for reference materials led us to analyze several petroleum shot cokes from a delayed coker unit, and, to the best of our knowledge, this is the first report of sulfur isotope composition of such materials. In delayed coking,[11] the heavy components from crude, typically a vacuum resid, are converted to coke through a semibatch process at temperatures of ∼425 °C. Nitrogen, sulfur, and metal contents of the coker feed are important parameters related to shot coke formation. High nitrogen, sulfur, and oxygen organic content encourages phase separation of the polynuclear aromatic (PNA) cores, with subsequent coking of these PNA cores in a locally restricted environment producing shot coke products. Consideration of isotope fractionation among petroleum components[5] suggests that the sulfur isotopes carried into the coke will be largely determined by values in the original crude. Because each crude can have a distinct isotope signature, such studies could aid in refining our understanding of how composition relates to coke morphology and fouling. An additional potential application of this work is the characterization of fouling coke deposits that form during combustion in internal combustion engines.

The microanalysis techniques described here were first documented in Lamberti et al.[12] The techniques as presented there are very general, intended for analysis of any material with a complex, heterogeneous matrix. Here, we provide greater details on the materials and methods that make this analysis optimal for analysis of solid organics. We focus here on a method to produce reliable sulfur isotope measurements by SIMS of solid organics.

1.1. Sulfur Isotope Geochemistry of Solid Bitumen.

Solid bitumen, present in many petroleum reservoirs, is an important part of petroleum geochemistry studies. This material can significantly impact oil reservoir quality. When present in large quantities, bitumen can occlude porosity and permeability, and, hence, degrade reservoir quality. If bitumen is overmature (i.e., fluid and gas depleted), it can incorrectly be identified as a hydrocarbon source, leading to overestimates of reserves (see ref 13 and references therein). When present in smaller amounts, it is still important as an indicator of paleo-geochemical conditions. Absent bacterial alteration, the $\delta^{34}S$ values[14] of kerogen and oil are generally ∼15‰ lower in ^{34}S values than the co-evolved sulfate.[5] For example, a sulfate value of $\delta^{34}S$ = +20‰ would coexist with a crude or kerogen of $\delta^{34}S$ = +5‰. If bitumen is the result of simple thermal alteration, the isotope ratio will remain similar, with some small shift, ∼2‰, to heavier values as light components are lost.

However, there are two key geochemical processes associated with oil reservoirs and source rocks that can significantly affect sulfur isotope ratios of the organic phase: bacterial sulfate reduction (BSR) and thermal sulfate reduction (TSR). Interest in these processes is due to the potential for creating sour-gas

Received: January 20, 2014
Revised: March 13, 2014
Published: March 14, 2014

   dx.doi.org/10.1021/ef5001776 | Energy Fuels 2014, 28, 2446−2453

Table 1. Hydrogen and XPS Analyses for Bitumen and Petroleum Coke

	Per 100 Carbon					Mole Percent		
sample	hydrogen[a]	total oxygen	aromatic carbon	total nitrogen	total sulfur	aliphatic sulfur	aromatic sulfur	sulfate
Petroleum Coke								
COKE1	60	3.5	78	2.5	1.7	0	93	7
COKE2	57	5.7	75	4.5	1.8	0	84	16
COKE3	52	4.7	78	3.3	2.0	0	89	11
COKE4	54	4.4	78	3.1	1.9	0	91	9
COKE5	55	4.8	82	3.2	1.6	0	89	11
COKE6	52	4.6	79	1.8	3.5	0	100	<1
Bitumen								
00DH90[b]	88	3.0	61	1.9	2.0	18	78	4
05DH046[b]	89	6.3	63	2.0	1.5	5	92	3
99DH12[b]	109	3.1	49	1.7	1.1	7	83	10

[a]Hydrogen measured by a combustion elemental analyzer. [b]Results from Kelemen et al.[13,33]

conditions. TSR is a potent source of H_2S, with attendant severe souring of the resulting hydrocarbon resource (see Machel et al.[5] for a discussion of the resulting isotope shifts). It is not the focus of the present paper to detail these trends; however, it is important to note that the magnitude of the isotope ratio shift is large. Powell and Macqueen[8] showed that the influx of TSR-derived sulfur shifts the bitumen sulfur isotope composition from its original +3‰ to +7‰ value to as high as +17‰. Another example is from SIMS analysis of pyrite and marcasite associated with the Nisku Formation. Riciputi et al.[15] have shown that both TSR and BSR processes are locally operative, finding a bimodal distribution of sulfur isotope ratios in those sulfides with peaks in the histogram at +15‰ and −20‰, interpreted as indicating formation by TSR and BSR, respectively. The overall conclusion is that sulfur isotope analyses are a useful tool in determining the impact of these processes, and moderate accuracy and precision are sufficient.

Although a useful geochemical indicator, a significant problem is the difficulty of extracting clean samples in sufficient quantities for conventional analysis. This is especially difficult when the bitumen is distributed as grain coatings. Thus, the high spatial resolution capabilities of SIMS make it an ideal tool for measuring isotope ratios in such solid materials. However, there are, to date, few examples of SIMS analysis of sulfur isotopes in solid organics. Unlike many mineral systems, satisfactory solid organic standards are not readily available. Carbon isotope ratios of organic matter have been measured by SIMS.[16−20] Recently, Bontognali et al.[9] undertook a SIMS study of sulfur isotopes in fossil remains of ancient microbial mats. Four Phanerozoic kerogen separates were examined to establish a matrix correction. A significant spread (>30‰ for a single sample) was found in SIMS isotope ratios for several of the kerogens. For such samples, the average does not equal the conventional bulk analysis value. Fortunately, one of their materials, kerogen from the Monterey Formation, exhibited a much smaller spread and had excellent agreement with the conventional value, providing a standard. Their observations show that the problem of inhomogeneous solid organic materials is widespread.

An objective of the present work is to illustrate a reliable SIMS matrix correction procedure, including both a material and a measurement protocol that will make SIMS measurement of sulfur isotope ratios for organic solids routine. As will be shown, the challenge in creating this approach is a lack of homogeneous standards. Intermixed with the sulfur-bearing organics are other sulfur-containing phases such as metal sulfides and sulfates. Although small in total mass, when using a high-spatial-resolution method, such as SIMS, the presence of such phases makes analyses challenging. This is especially true for a SIMS standard that will be analyzed before and after every unknown analysis session, where reliable homogeneity is required. We demonstrate a successful strategy to overcome this, and we identify petroleum coke and solid bitumen standards that are useful in such geochemical analyses.

1.2. SIMS Mass Bias Effects: Instrument Mass Fractionation (IMF) and Matrix Correction. A long-standing challenge of SIMS is correcting for isotopic fractionation introduced during sputtering and transmission of secondary ions.[21] This can be envisioned as two mechanisms that cause fractionation of the observed isotope ratio from the true value in the solid matrix. First, an instrument-dependent isotopic mass fractionation occurs during transmission of secondary ions through the ion optics and mass spectrometer. This will vary with analytical conditions such as tuning of the instrument. We refer herein to this type of fractionation as instrument mass fractionation (IMF). Second, as a result of the sputtering process, a matrix-dependent isotopic fractionation occurs during ion generation as a result of the sputtering process. This effect will, of course, also be dependent on experimental conditions, such as incident ion beam energies, beam flux, and primary ion choice (e.g., $^{133}Cs^+$ versus $^{16}O^-$). However, if these factors are held constant, the resulting correction is highly sensitive to the chemical composition and structural bonding environment of the element of interest within a given matrix. We refer herein to these chemical effects as the matrix effect.[21−23] Matrix effects can be large, and offsets of the isotope ratio from the true value of more than 10 parts per thousand are common. Empirical corrections have been proposed,[24,25] but these have limited utility, because of the need of highly accurate isotope ratios for most applications.[26]

Conventionally, the IMF and matrix corrections are made simultaneously through analysis of a well-characterized, homogeneous standard that matches the chemical composition and structure of the unknown. The geochemical literature offers many examples where researchers have carefully developed standards as part of their use of SIMS.[19,25,27−29] Here, we develop standards for sulfur isotope analysis from organic solids and demonstrate an approach to utilize these inhomogeneous standards.

1.3. Strategies and Standards for IMF and Matrix Correction. Lacking a homogeneous standard, an alternative

dx.doi.org/10.1021/ef5001776 | Energy Fuels 2014, 28, 2446−2453

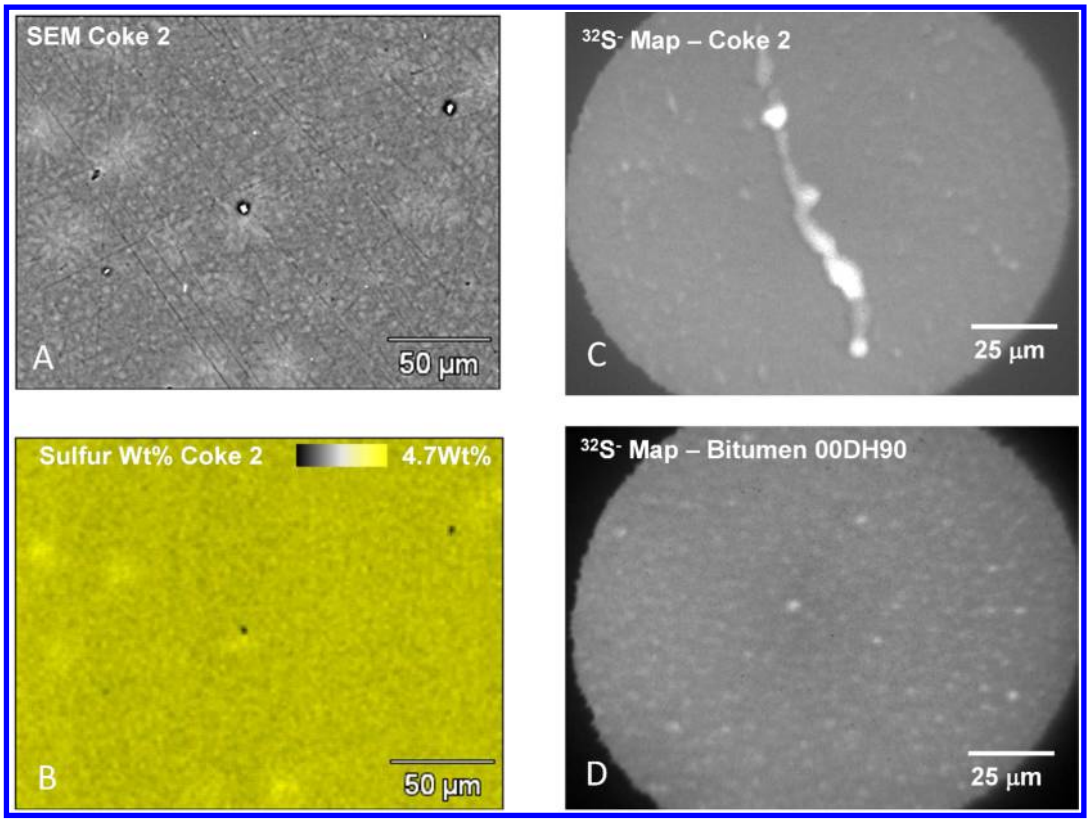

Figure 1. Typical compositional features of solid organics that present challenges to spatially resolved sulfur isotope analyses. (A) Electron backscattered image of COKE2 from scanning electron microscopy (SEM); brighter areas are local concentrations of sulfur and alkali metals. (B) Sulfur compositional variation of COKE2 from electron dispersive analysis. (C) SIMS image of $^{32}S^-$ from COKE2 showing the distribution of secondary phases. The majority of the sample contains organic sulfur (gray region). Brighter regions, such as the filamentous region in the center and the small, dispersed specks throughout the matrix represent contaminants. (D) SIMS image of $^{32}S^-$ from 00DH90 bitumen; abundant small dispersed minor phases are observed.

approach is to utilize a separate IMF standard and then apply a matrix correction factor. This is an approach analogous to that used by Page et al.[30] for compositional analysis of titanium in zircon. A NIST glass was used as a running standard to normalize the SIMS measured $^{49}Ti/^{30}Si$ data. Then, using several synthetic Ti-doped zircons, they derived a separate matrix correction: a relative sensitivity factor (RSF). This RSF applied to the SIMS corrected $^{49}Ti/^{30}Si$ data produced accurate Ti contents for zircon.

Here, we first select a standard for the IMF correction alone. For sulfur, we used standard[31] IAEA_S1, with $\delta^{34}S = -0.30 \pm 0.03‰$, and an in-house sample, Ald_AG2S (a pressed powder of >99.9% pure Ag_2S) with $\delta^{34}S = 1.77 \pm 0.24‰$, which was calibrated through multiple ($n = 5$) conventional analyses. For the matrix correction standard, requiring similarity in chemical bonding environment to bitumen, i.e., aromatically bonded sulfur in a carbonaceous matrix having H/C in the range of 0.2−1, we identified shot coke produced from a delayed coker unit as having the required chemistry. Having determined that the range of sulfur isotope ratios in these coke samples was somewhat limited, we added three solid bitumens collected from exposed veins in the North Slope region of Alaska, formed by thermochemical alteration (TCA).[13]

Unfortunately such materials are inhomogeneous. To successfully utilize such a standard, a meaningful comparison between conventional, bulk mass spectrometry and SIMS analysis is required. For coke, these inhomogeneities are minor secondary phases (<10%, see Table 1) that form during high-temperature annealing. Our strategy was to develop an approach to produce SIMS data that rejected or down-weighted impurity-affected analyses. By doing so, we produce a dataset that can be compared with the conventional analyses, thus producing a reliable matrix correction for the SIMS isotope ratios. Furthermore, multiple standards can be used in this scheme to increase confidence in the correction and to account for any possible compositional dependence of a matrix effect correction. Through a matrix correction that includes multiple standards, a straightforward regression analysis can produce a widely useful calibrated matrix correction.

For an analytical session, we perform multiple analyses of the IMF standard, establishing the IMF correction for that session, and then analyze the unknowns. We first apply the IMF correction, producing a value we designate as $\delta^{34}S_{SIMS\text{-}IMF}$. Then, the calibrated matrix correction is applied to this value, resulting in the unbiased isotope ratio for the unknown, $\delta^{34}S_{V\text{-}CDT}$. Analytical precision is estimated by propagating uncertainties. Using the familiar formulation for uncorrelated Gaussian errors, we calculate $\sigma^2 = SE^2 + \sigma_m^2$, where SE^2 is the experimental standard error (calculation details given section 3.2.1, "Outlier Rejection") and σ_m^2 is the estimated uncertainty from linear regression determination of the matrix correction.

2. EXPERIMENTAL SECTION

We used a variety of techniques to analyze the sample chemistry. For these predominately carbonaceous solids, X-ray photoelectron spectroscopy (XPS) provides a good measure of overall composition and

dx.doi.org/10.1021/ef5001776 | Energy Fuels 2014, 28, 2446−2453

Table 2. Conventional and SIMS Results from Solid Organics

sample	type	Conv. $\delta^{34}S$ (‰,V-CDT)[a]	Outlier Rejection $\delta^{34}S_{SIMS\text{-}IMF}$ (‰)[b]	$\delta^{34}S_{V\text{-}CDT}$ (‰)[c]	Bartlett test $\delta^{34}S_{SIMS\text{-}IMF}$ (‰)[d]	weighted mean $\delta^{34}S_{SIMS\text{-}IMF}$ (‰)[e]
Organic Standards						
COKE1	coke	8.90 ± 0.30	32.1 ± 0.49[f]	8.6 ± 0.50	32.1 ± 0.86	32.0 ± 0.64
COKE2	coke	7.20 ± 0.42	31.1 ± 0.57	7.6 ± 0.59	31.1 ± 0.85	31.2 ± 0.84
COKE3	coke	4.05 ± 0.30	27.3 ± 0.47	3.8 ± 0.55	27.5 ± 1.40	27.8 ± 0.58
COKE4	coke	2.00 ± 0.30	24.9 ± 0.39	1.4 ± 0.54	24.7 ± 1.11	24.3 ± 0.48
COKE5	coke	−4.30 ± 0.28	20.1 ± 0.32	−3.4 ± 0.41	19.5 ± 1.27	19.4 ± 0.45
COKE6	coke	−5.70 ± 0.30	17.8 ± 0.50	−5.7 ± 0.57	17.6 ± 1.19	17.5 ± 0.6
00DH90	bitumen	−20.27 ± 0.30	2.5 ± 0.37	−21.0 ± 0.49	0.9 ± 0.66	1.0 ± 0.54
05DH046	bitumen	−17.93 ± 0.58	6.5 ± 0.48	−17.0 ± 0.57	6.8 ± 4.61	8.1 ± 0.63
99DH12	bitumen	−12.53 ± 0.30	10.4 ± 0.48	−13.2 ± 0.54	10.4 ± 2.01	3.9 ± 0.65

[a]Values from EA-IRMS analysis,[35] estimated precision (0.3) or SD of multiple analyses indicated. [b]Truncated mean formed from analysis of entire population using Otsu's method. [c]Calculated from recommended model $\delta^{34}S_{V\text{-}CDT} = A + \delta^{34}S_{SIMS\text{-}IMF}B$, where $B = 1$ and $A = -23.5 \pm 0.29$‰. [d]From subset of data. Rejected analyses SE > reference value, where value is set by use of Bartlett test at a 95% onfidence interval. [e]Contributions to average are weighted by 1/(standard error)^2. [f]One SE shown.

bonding type. Establishing the sulfur bonding environment is a key element in developing a SIMS matrix correction, with aromatic bonding best matching that in solid bitumen. Descriptions of the XPS methods for the analysis of oxygen, carbon, nitrogen and sulfur are found in Walters et al.[32] and Kelemen et al.[13,33] Briefly, solid bitumen and petroleum coke were analyzed with a Kratos Axis Ultra XPS system, using monochromatic Al Kα radiation. The analysis area was a ~400 μm^2 elliptical region (set by the photoelectron analyzer acceptance area). The unit is equipped with automatic sample charge neutralization to ensure a uniform sample space charge. The elemental concentrations are reported (Table 1) relative to carbon, calculated from XPS spectra based on the area of the characteristic photoelectron peaks after correcting for atomic sensitivity. The sulfur content of the samples ranges over 1.1−3.5 S/C atomic ratio, corresponding to ~3−9 wt %. Sulfur is mainly organically bound, with a minor sulfate component.

Minor inorganic impurities are also present, and previous analyses show that the most common metals include calcium, vanadium, iron, and nickel (typical ~500 ppm), associated with porphyrins in the original feed or with sulfates formed during the coking process.[11,34] Obviously, the sulfates contaminates are our focus here.

In the Brooks Range TCA solid bitumen, nickel and vanadium associated with porphyrins are present at levels similar to asphaltenes (Ni ≈ 300−450 ppm) and (V ≈ 500−1750 ppm).[33] From sulfur X-ray absorption extended fine structure (XANES) studies on these samples,[13] we conclude that metal sulfides (most likely pyrite) are also present at low levels, 0.02−0.04 mol fraction of the total sulfur. The minor sulfate and aliphatic sulfur has been attributed to a variety of possible origins,[13,33] including deposition and/or diagenesis of precursory bitumen material, TCA processes, or possibly surficial weathering.

Having confirmed the essentially carbonaceous nature of the matrix, we characterized the impurity distribution within that matrix using SIMS imaging, complemented by scanning electron microscopy (SEM) and electron microprobe analysis (EMPA). The primary goal of this work was to establish the length scale of the impurities, aiming to focus SIMS analysis on the homogeneous regions. For this, SIMS imaging was our main tool. As applied, we have excellent sensitivity to low levels of impurity (several ppb), but composition is qualitative because ion yield will vary from matrix to matrix. A survey of results is given in Figure 1, showing enhanced $^{32}S^-$ ion yield from impurities (see Figures 1C and 1D). Tuning to other masses, we find that these impurities are associated with metals such as iron, nickel, and calcium. To better quantify the range of inhomogeneity, we selectively analyzed several of our samples using SEM and EMPA, with a typical example shown in Figures 1A and 1B. The structure here highlights the typical mosaic/domain structure of coke.[11] The high contrast regions in the SEM backscattered election image are correlated with EMPA analysis, showing that these are zones of elevated sulfur. These same regions also have elevated concentrations of vanadium. We show this example, to indicate how we target our SIMS analysis (8 μm diameter region), focusing on the surrounding homogeneous zones.

These analyses showed that (1) the sulfur bonding is favorable for their use as solid organic standards, (2) the overall level of impurities is low, and (3) that microimaging can be used to avoid many impurities. However, SIMS analysis indicates that unresolved impurities also contribute to the data. Given that the origin of the impurities is inherent to the material formation; this is a problem best addressed through post-processing data analysis, which is the focus of the remainder of this work.

For SIMS analysis, individual pieces of bitumen and petroleum coke were crushed into small (<4 mm) chips, mounted in low-sulfur epoxy (Buehler Epo-Thin, ~300 ppm sulfur), and polished using SiC polishing paper and diamond suspension. Three to five chips were mounted in each metal sample holder, and all were positioned near the center of that circular ring. Prior to analysis, mounts were coated with 25−30 nm of gold. Charge neutralization via an electron flood gun was not available, thus sample charging was controlled by painting a graphite suspension along the edges of grains and to the edge of the metal sample holder. For most samples this was adequate. If a sample exhibited beam instability typical of charging, a copper TEM grid with 100 μm square grid spacing was secured to the top of gold-coated grains with double-sided carbon tape, and then graphite was painted from the grid to the edge of the metal sample holder. In these cases, analyses were performed in the spaces between lines of the copper grid.

SIMS analyses were performed on a Cameca IMS 3f at the ExxonMobil Research and Engineering Company. For a detailed description of the optics of the IMS 3f, see the work of Ireland.[22] An ~40 nA Cs^+ primary beam with an impact energy of 14.5 keV was directed onto the sample through lenses 1 and 2, followed by a primary beam aperture. Negative secondary ions were collected from the sample through an optic train consisting of immersion and transfer lenses, contrast aperture, entrance slit, field aperture, and energy slit prior to the mass spectrometer and an exit slit before the electron multiplier ion detector (SGE Analytical Science). Specific settings for imaging and HMR analyses are given below. Charge neutralization was achieved using the aforementioned techniques.

When analyzing a sample, SIMS imaging was first employed with the transfer lens set to 150 μm, and the contrast (20 or 50 μm) and field apertures (400 μm) set to give an image with higher lateral resolution at the expense of mass resolution. This image was projected onto a CCD camera located downstream from the mass spectrometer. Prior to sulfur isotope analysis, careful SIMS imaging of $^{12}C^-$, $^{16}O^-$,

dx.doi.org/10.1021/ef5001776 | Energy Fuels 2014, 28, 2446−2453

$^{32}S^-$, and $^{34}S^-$ was used to identify and avoid resolvable inhomogeneities.

For isotope ratio analysis, we switched to high-mass-resolution conditions, typically ≥4000 mass resolving power to avoid molecular interference such as ^{32}S from $^{16}O_2$. The transfer lens (150 μm) and field aperture (100 μm) were set such that only ions extracted from the central 8 μm of the sputtered crater were analyzed. Extracted secondary ions were not filtered for energy, and the source and exit slit settings were optimized to remove undesired isobaric interferences and to tolerate slight beam shifts of the secondary ion beam during magnet cycling. Ions were measured by magnetic peak switching. Each analysis consisted of 50 cycles of counting ^{32}S for 1 s and ^{34}S for 5 s at a count rate of ~2 × 10^5 counts per second for ^{32}S. We follow the nomenclature of Fitzsimmons et al.[35] throughout this work, and from that work, these 50 measurements make up one analysis. A few early data points were taken with 25 cycles, noted by a slightly larger SE. The sample was sputtered for 3−5 min to reach a steady count rate prior to beginning data collection. A dead-time correction was applied, following the techniques of White and Wood[36] and Fahey.[37] Counting statistics of a single analysis leads to an estimated relative standard error of the mean (RelSE, equivalent to $e_{\bar{x}}$ from Fitzsimons et al.[35]) of 0.74‰. The two IMF standards, measured over a period of several months in this study, give a mean value for this same quantity for over 120 analyses: $RelSE_{std}$ = 1.10 ± 0.03‰ (±1 SE indicated). This value somewhat exceeds counting statistics, suggesting that there are other factors influencing the precision such as instrument instabilities, electronic noise, or minor charging. This value, $RelSE_{std}$, will provide an important baseline when we analyze the SIMS results from the solid organic standards.

3. RESULTS AND DISCUSSION

3.1. Isotopic Characterization of Standards. We obtained the bulk isotopic composition of the six cokes and three bitumens standards via conventional techniques. These results were obtained through conventional EA-IRMS methods at Isotech Laboratories, Inc. (see Table 2).[38] The resulting values of $\delta^{34}S_{V\text{-}CDT}$ for the cokes and bitumens range from +9‰ to −20‰. Replicate analyses ($n \geq 3$) yielded a reproducibility of ±0.3‰ (1SD), which is commensurate with the uncertainty of the technique, with the exception of COKE2 (±0.4‰ 1SD) and bitumen 05DH-046 (±0.6‰ 1SD). The good reproducibility of replicate sample analysis suggests that heterogeneities are uniformly distributed at the scale of the bulk measurements (several milligrams of sample).

To gauge the impact of heterogeneities on the bulk isotope values, we consider their likely isotopic composition. Thermodynamic fractionation, governing the isotope fractionation between reduced and oxidized sulfur forms, varies[39] as ~constant/T^2. Consequently, at the high temperatures of the delayed coker unit (~425 °C), fractionation of $^{34}S/^{32}S$ is likely low. The fractionation equation for TSR[5] gives an estimate for this, and we calculate a slight enrichment in the sulfate for ^{34}S, i.e., $\Delta^{34}S \equiv \delta^{34}S_{sulfate} - \delta^{34}S_{organic}$ = +0.7‰. Taking this value and using the sample with the largest sulfate content, COKE2, we calculate that the reported $\delta^{34}S$ = 7.2‰ value would only be shifted to 7.1‰ if the sample were to have been purely organic sulfur, within the reported uncertainties of SIMS measurements. Given the significant uncertainty in the origin of the sulfur impurities in the Brooks Range bitumen,[13,33] we are unable to suggest an isotope composition model. However, two samples have low sulfate contents and the sample 99DH12, with highest sulfate content, does not significantly differ in agreement between SIMS analysis and bulk isotope values, suggesting that our inclusion of these samples is valid. Therefore, our conventional analyses adequately reflect the sulfur isotopes of the organic phase, and our challenge is to produce SIMS data that also do so.

3.2. Addressing Sample Heterogeneities. Addressing the chemical and isotopic heterogeneity during SIMS analyses played a major role in this study. In common with standard practice within the community, careful selection of the sampling area and a post-processing of data were used. The first step was to sample the most homogeneous region, and SIMS imaging was the principal guide, with the analyst avoiding obvious impurities; however, it is clear that small scale impurities are also present (note the small bright areas in the SIMS images shown in Figure 1). Post-analysis examination of the sputtering crater is of limited use. Postanalysis screening for impurities is imprecise because the few square micrometer region from which the ions are extracted is much smaller than the sputtered region (an elliptical footprint with dimensions of ~0.2 mm × 0.3 mm). We rejected any data showing an impurity or sample discontinuity, such as a crack. However, the resulting data still exhibited significant interanalysis and intra-analysis variation, indicating that further processing was required.

Consider how the presence of impurities will affect the analysis. Even though the regions that are purely contaminants are excluded, during the sputtering process, we may encounter an impurity that was not present at the sample surface. The ion yield at that point will consist of contributions from a solid organic and an impurity. We have argued that the organic and oxide impurities will generally be within $\Delta^{34}S \approx 0.7‰$; however, the effect here could be larger, because of different ion yields from the two matrices. This will produce an outlier in the $^{34}S/^{32}S$ ratio. If the outliers were distributed equally about the mean isotope ratio of the organic, a large number of observations would minimize their impact. This assumption is questionable here, and that is confirmed in the next section. Of course, detection of the outlier at the time of an individual measurement would be desirable. However, the precision from counting statistics is 5.2 ‰ for a single measurement cycle (eq 21, see Fitzsimons et al.[35]). Thus, rejection at a 95% confidence interval (~2SD) would not generate high precision analyses. Several strategies for post-analysis outlier detection and rejection are discussed below.

3.2.1. Outlier Rejection. As Fitzsimons et al.[35] has shown the population of all SIMS measurements from a single homogeneous material follows an approximately normal distribution. See, for example, their Figure 3 and our Figure 2A. Shown in Figure 2A is a Q−Q plot[40] that compares the quantiles of the IAEA_S1 sample measurements (recalling our definitions earlier: 2350 measurements taken over 47 analyses) with a standard normal distribution. The linearity of the values indicates that the IAEA_S1 data are, as expected, normally distributed, extending for ~4σ width around the mean value.

Sample impurities are expected to produce deviations from a unimodal distribution in the $^{34}S/^{32}S$ ratio. An example is shown by the Q−Q plot of measurements from sample 99DH12 (900 data) in Figure 2B. Two linear regions signal a bimodal distribution.

Assuming that true isotope ratios and outliers are both normally distributed with different means and variances (which is borne out by a visual examination of the data from a few representative samples), the problem of outlier rejection becomes one of finding a threshold τ^* that separates two−possibly overlapping−normal distributions in some optimal fashion. One method of separating two distributions, originally

dx.doi.org/10.1021/ef5001776 | Energy Fuels 2014, 28, 2446−2453

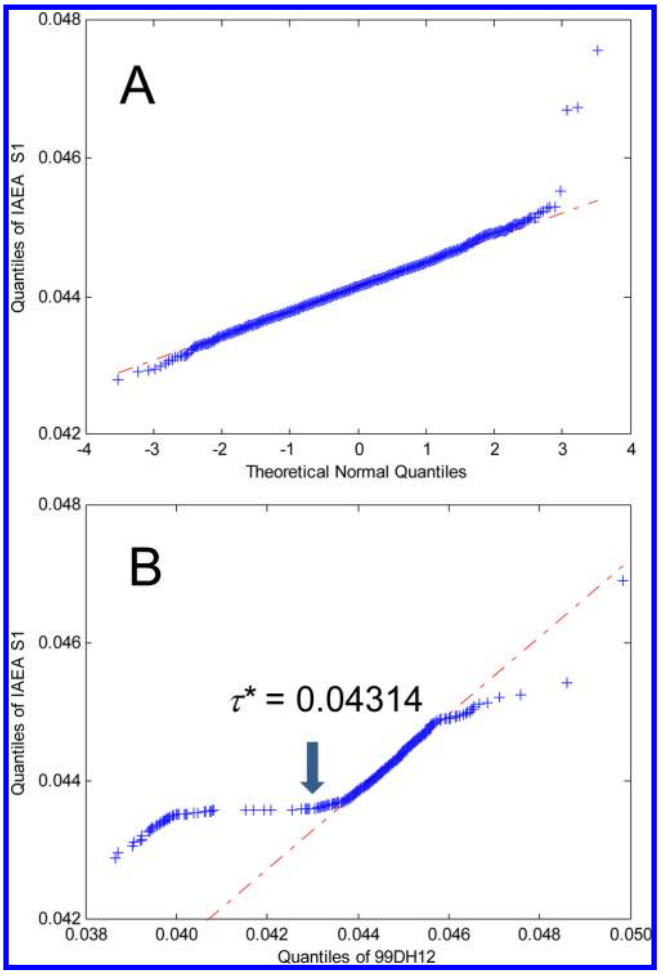

Figure 2. (A) Q–Q Plot of IAEA_S1 sample measurements (2350 data taken over 47 analyses) versus the theoretical quantiles for a normal distribution. The linearity shows that these data, as expected for a homogeneous sample, are normally distributed. (B) Sample 99DH12 (900 data) exhibits a bimodal distribution with outliers at smaller isotope ratios. Outlier rejection (see text) results in the rejection of data below τ^* (65 data eliminated). The resulting mean isotope ratio, 0.044616 ± 0.00045 (which after matrix correction gives $\delta^{34}S_{V\text{-}CDT} = -13.23 \pm 0.54‰$), corresponds to within 2SE of the value from conventional analysis (−12.53 ± 0.3‰).

proposed by R. A. Fisher,[41] is to find the threshold that maximizes the ratio of the squared distance between the means to the variance within each distribution, i.e.,

$$\tau^* = \text{argmax}_{\tau} \frac{(\mu_{<\tau} - \mu_{>\tau})^2}{\sigma_{<\tau}^{\ 2} + \sigma_{>\tau}^{\ 2}}$$

where $\mu_{<\tau}$ and $\sigma_{<\tau}^{\ 2}$ (and, similarly, $\mu_{>\tau}$ and $\sigma_{>\tau}^{\ 2}$) are, respectively, the mean and variance calculated from the observations with $^{34}S/^{32}S$ value less than (greater than) τ^*. This measure is commonly used in statistics,[42] since it minimizes the expected risk for an incorrect classification and can be computed using Otsu's algorithm.[43]

Applying this procedure to the 99DH12 example causes ∼7% of the observations to be rejected (65 of the 900 data) for τ^* = 0.04314, improving agreement of the quantiles with that of the homogeneous standard and giving a mean value significantly shifted from that of the entire dataset, respectively:

Truncated Mean = 0.044616 ($\delta^{34}S_{SIMS\text{-}IMF}$ = 10.4‰, Table 2)

versus

Overall Mean = 0.044313 ($\delta^{34}S_{SIMS\text{-}IMF}$ = 3.4‰)

We apply one final step to calculate the SE without assuming complete normalcy of the distribution. Using a bootstrapping procedure,[44] multiple resamples of the truncated data yield a distribution of resample means (100 in this case). The standard deviation of this distribution is a robust estimate of the true SE. The resulting values are reported in Table 2.

3.2.2. Bartlett Test. The Bartlett test provides a means to test if a SE is larger than expected. Here, we identify the increase in SE for a given analysis with the inclusion of outliers among the set of 50 measurements. We apply a χ^2 test to reject those affected analyses. The IMF standard provides a measure of the expected value for the unperturbed SE under our instrument conditions, $RelSE_{std}$ = 1.10 ± 0.03‰. A distinct advantage is that this test can be performed immediately upon completion of a single analysis, but it is susceptible to some bias if data are non-normally distributed. The results here are comparable to the results from section 3.2.1, "Outlier Rejection", suggesting that this is not a significant problem.

Following the procedures for testing multiple populations for equivalence variance,[45,46] we construct the following test. For a given analysis of the solid organic, we calculate the relative SE over 50 measurements, designated as $RelSE_{sam}$, sample size 50. This value is compared to $RelSE_{std}$ for the IMF standards (sample size = 120 × 50). We reject the null hypothesis for this paired comparison, $RelSE_{std} = RelSE_{sam}$, at a 95% confidence level through a $\chi_{1-\alpha,k}^{\ 2}$ statistic, where $1 - \alpha = 0.95$ and $k = 1$. This gives a numeric cutoff for our analyses of $RelSE_{sam} < 1.327$, designated as $>RelSE_{std}$ criterion throughout this work. From the over 150 analyses, this rejection criterion excludes about 50 data. The resulting mean and SE for each of the nine samples are shown in Table 2, with details given in the Table A1 in the Supporting Information.

3.2.3. Weighted Mean. A third method tested was to form a weighted mean for each sample. The average values are calculated using a weighting for each analysis of $w_i = SE_i^{-2}/\sum_1^N SE_n^{-2}$, where SE is the standard error of the mean from that analysis, and the sum is carried out for all analyses of a single sample. The weighted means are shown in Table 2 and in Table A1 in the Supporting Information.

3.3. Recommended Matrix Correction. We obtain the matrix correction through linear regression of IMF-corrected SIMS data ($\delta^{34}S_{SIMS\text{-}IMF}$) versus the conventional analyses values. Using the $\delta^{34}S_{SIMS\text{-}IMF}$ values from section 3.2.1, "Outlier Rejection" and weighting each value by $w_i = 2SE_i^{-2}$, we obtained best estimates for the variables in the following equation: $\delta^{34}S_{V\text{-}CDT} = A + \delta^{34}S_{SIMS\text{-}IMF}B$, as follows: A= −23.4 ± 0.60‰ and B = 0.99 ± 0.03 with R^2 = 0.99785. The B value is not statistically significant, thus we set B = 1 and obtained our recommended model for the calibrated matrix correction, $\delta^{34}S_{V\text{-}CDT} = -23.5 \pm 0.29‰ + \delta^{34}S_{SIMS\text{-}IMF}$, shown in Figure 3.

As Figure 3 shows, the agreement between this model and the conventional analyses is very good; all values agree within 2SE.

To compare the accuracy of outlier rejection for all methods, we calculated the following statistic: $s^2 = \sum(\delta^{34}S_{V\text{-}CDT} - \text{Conv.}\delta^{34}S)^2$. Applying this to the results for the four conditions—(1) mean of all analyses, (2) outlier rejection, (3) Bartlett test, and (4) weighted mean—gives s = 7.8‰ s = 1.8‰, s = 3.1‰, and s = 7.9‰, respectively. As expected, the outlier rejection method gives the best outcome, with the

dx.doi.org/10.1021/ef5001776 | Energy Fuels 2014, 28, 2446−2453

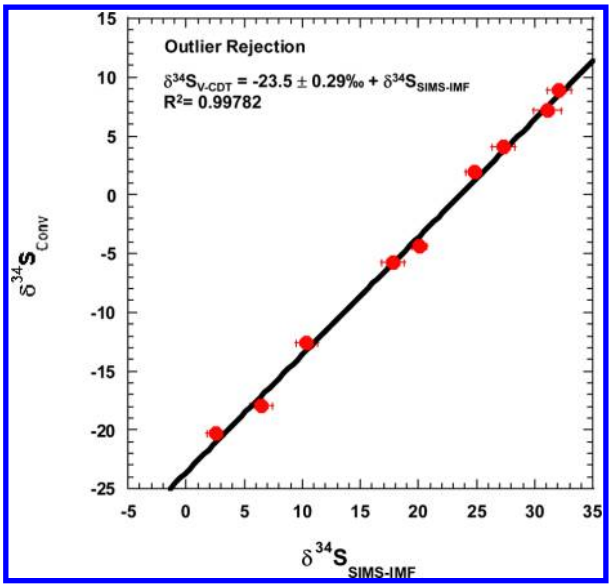

Figure 3. Plots showing average $\delta^{34}S_{SIMS\text{-}IMF}$ values versus $\delta^{34}S_{V\text{-}CDT}$ from conventional mass spectrometry (EA-IRMS). The $\delta^{34}S_{SIMS\text{-}IMF}$ values come from the Outlier Rejection method described in the text. Mean values along with ±2SE are plotted. Weighted, least-squares analysis yields the results shown and plotted as a solid line. This equation allows IMF corrected SIMS data taken on solid organics to be converted to matrix-corrected values.

average deviation from the Bartlett test being nearly twice as large. The weighted mean method gives poor agreement, showing that the removal of outliers is important.

We recently applied these techniques to an analysis of the variation of sulfur isotopes in solid bitumen from the Big Piney-La Barge Production Complex.[10] As expected, a change in SIMS operating conditions caused a slight shift in the value of our calibrated matrix value, *A*. This was calibrated through the use of COKE2 from the present study. Regardless, the approach was successful in identifying two isotopically distinct sulfur sources that were subsequently altered by TSR processes.

4. CONCLUSIONS

Here, we demonstrate a robust protocol for secondary ion mass spectrometry (SIMS) analysis of sulfur isotopes in solid organics. This includes identification of petroleum coke as an excellent standard as well as procedures to minimize the impact of inhomogeneities inherent in these materials. Because sulfur isotopes can provide key data indicting origin and formation conditions, we anticipate that use of this protocol will facilitate important analyses of solid organics.

To the best of our knowledge, the data here on sulfur isotopes in petroleum coke are among the first reported in the literature. The $\delta^{34}S$ range from −5.7‰ to 8.9‰ and reflect the combined effects of petroleum source variation and coking-induced changes. Sulfur is incorporated into kerogen during early diagenesis through bacterial reduction of sulfate. The $\delta^{34}S$ of the organic sulfur results from the extent of biological fractionation and the value of the sulfate, which varies over geologic time. Typically, the $\delta^{34}S$ of whole oils are offset by approximately −15‰ from the marine sulfate.[2,5] This accounts for the majority of the reported variation in crude oil $\delta^{34}S$ values ranging from −10‰ to +35‰, with some additional variation imparted by local depositional conditions.[1] Alternatively, sulfur may be incorporated into oil by thermochemical sulfate reduction, which is an abiotoic process that can occur in high-temperature reservoirs. The coke materials measured here span a more-restricted sulfur isotope range than the crude values from Thode et al.[1] However, they are consistent with expected petroleum source variations across the Phanerozic.

This study focuses on sulfur in organic solids, but the approach is applicable to any isotope and matrix combination, whenever a single isotope measurement of a heterogeneous reference sample is not representative of the bulk composition. The techniques we developed here can be widely employed when doing SIMS analyses and is a method that will prove useful in analyzing many types of organic solids and other complex matrices.

■ ASSOCIATED CONTENT

Ⓢ Supporting Information

Sulfur isotope compositions of bitumens and petroleum coke (Table A1). Data rejected by the Bartlett Test are marked in red. This material is available free of charge via the Internet at http://pubs.acs.org.

■ AUTHOR INFORMATION

Corresponding Author

*Tel.: 908-730-2888. E-mail: hubert.e.king@exxonmobil.com.

Present Address

[†]Los Alamos National Laboratory, P.O. Box 1663, Los Alamos, NM 87545, USA.

Notes

The authors declare no competing financial interest.

■ ACKNOWLEDGMENTS

Our thanks to Simon Kelemen for his insight into solid organic chemistry and for his providing the coke and bitumen samples, and to he and Peter Kwiatek for the XPS analyses. We thank Clifford Walters, Robert Pottorf, and Gordon Macleod for their insights into sulfur geochemistry and the importance of solid bitumen in petroleum geochemistry.

■ REFERENCES

(1) Thode, H. G.; Monster, J.; Dunford, H. B. *Am. Assoc. Pet. Geol. Bull.* **1958**, *42* (11), 2619−2641.
(2) Krouse, H. R. *J. Geochem. Explor.* **1977**, *7*, 189−211.
(3) Thode, H. G. *AAPG Bull.* **1981**, *65*, 1527−1535.
(4) Orr, W. L.; Sinninghe Damsté, J. S. In *Geochemistry of Sulfur in Fossil Fuels*; Orr, W. L., White, C. M., Eds.; American Chemical Society: Washington, DC, 1990; pp 2−29.
(5) Machel, H. G.; Krouse, H. R.; Sassen, R. *Appl. Geochem.* **1995**, *10* (4), 373−389.
(6) Aharon, P.; Fu, B. *Geochim. Cosmochim. Acta* **2000**, *64* (2), 233−246.
(7) Cai, C.; Zhang, C.; Cai, L.; Wu, G.; Jiang, L.; Xu, Z.; Li, K. *Chem. Geol.* **2009**, *268* (3−4), 197−210.
(8) Powell, T. G.; Macqueen, R. W. *Science* **1984**, *224*, 63−65.
(9) Bontognali, T. R. R.; Sessions, A. L.; Allwood, A. C.; Fischer, W. W.; Grotzinger, J. P.; Summons, R. E.; Eiler, J. M. *Proc. Natl. Acad. Sci.* **2012**, *109* (38), 15146−15151.
(10) King, H. E., Jr.; Walters, C. C.; Horn, W. C.; Zimmer, M.; Heines, M.; Lamberti, W. A.; Kliewer, C.; Pottorf, R. J.; Macleod, G. *Geochim. Cosmochim. Acta* **2013**, http://dx.doi.org/10.1016/j.gca.2013.11.005.
(11) Siskin, M.; Kelemen, S. R.; Eppig, C. P.; Brown, L. D.; Afeworki, M. *Energy Fuels* **2006**, *20* (3), 1227−1234.
(12) Lamberti, W.; King, H.; Horn, W.; Zimmer, M.; Macleod, G.; Pottorf, R.; Srnka, L. Eur. Pat. Appl. WO2011136858 A1, 2011.

(13) Kelemen, S. R.; Walters, C. C.; Kwiatek, P. J.; Freund, H.; Afeworki, M.; Sansone, M.; Lamberti, W. A.; Pottorf, R. J.; Machel, H. G.; Peters, K. E.; Bolin, T. *Geochim. Cosmochim. Acta* **2010**, *74* (18), 5305−5332.
(14) All sulfur isotope ratios here are given in the conventional nomenclature as follows: $\delta^{34}S$ = 1000(($^{34}S/^{32}S$) sample/($^{34}S/^{32}S$) CDT)-1, where the reference value of Canyon Diablo Troilite ($^{34}S/^{32}S$)CDT is defined by the requirement that IAEA_S1 $\delta^{34}S$ = −0.3.
(15) Riciputi, L. R. *Geochim. Cosmochim. Acta* **1996**, *60* (2), 325−336.
(16) Fletcher, I. R.; Kilburn, M. R.; Rasmussen, B. *Int. J. Mass Spectrosc.* **2008**, *278* (1), 59−68.
(17) House, C. H.; Schopf, J. W.; McKeegan, K. D.; Coath, C. D.; Harrison, T. M.; Stetter, K. O. *Geology* **2000**, *28* (8), 707−710.
(18) Lepot, K.; Williford, K. H.; Ushikubo, T.; Sugitani, K.; Mimura, K.; Spicuzza, M. J.; Valley, J. W. *Geochim. Cosmochim. Acta* **2013**, *112*, 66−86.
(19) Sangely, L.; Chaussidon, M.; Michels, R.; Huault, V. *Chem. Geol.* **2005**, *223* (4), 179−195.
(20) Williford, K. H.; Ushikubo, T.; Schopf, J. W.; Lepot, K.; Kitajima, K.; Valley, J. W. *Geochim. Cosmochim. Acta* **2013**, *104*, 165−182.
(21) Shimizu, N.; Hart, S. R. *J. Appl. Phys.* **1982**, *53*, 1303−1311.
(22) Ireland, T. R., SIMS Measurement of Stable Isotopes. In *Handbook of Stable Isotope Analytical Techniques*; de Groot, P. A., Ed.; Elsevier: Amsterdam, 2004; Vol. *1*, pp 652−691.
(23) Riciputi, L. R.; Paterson, B. A.; Ripperdan, R. L. *Int. J. Mass Spectrosc.* **1998**, *178* (1−2), 81−112.
(24) Eiler, J. M.; Graham, C.; Valley, J. W. *Chem. Geol.* **1997**, *138* (3−4), 221−244.
(25) Hauri, E. H.; Shaw, A. M.; Wang, J. H.; Dixon, J. E.; King, P. L.; Mandeville, C. *Chem. Geol.* **2006**, *235* (3−4), 352−365.
(26) Valley, J. W.; Kita, N. T., In Situ Oxygen Isotope Geochemistry by Ion Microprobe. In *Secondary Ion Mass Spectrometry in the Earth Sciences*, Fayek, M., Ed.; Mineralogical Association of Canada: Quebec, 2009; Vol. *41*, pp 19−63.
(27) Kozdon, R.; Ushikubo, T.; Kita, N. T.; Spicuzza, M.; Valley, J. W. *Chem. Geol.* **2009**, *258* (3−4), 327−337.
(28) Black, L. P.; Kamo, S. L.; Allen, C. M.; Davis, D. W.; Aleinikoff, J. N.; Valley, J. W.; Mundil, R.; Campbell, I. H.; Korsch, R. J.; Williams, I. S.; Foudoulis, C. *Chem. Geol.* **2004**, *205* (1−2), 115−140.
(29) Kelly, J. L.; Fu, B.; Kita, N. T.; Valley, J. W. *Geochim. Cosmochim. Acta* **2007**, *71* (15), 3812−3832.
(30) Page, F. Z.; Fu, B.; Kita, N. T.; Fournelle, J.; Spicuzza, M.; Schulze, D. J.; Viljoen, F.; Basei, M. A. S.; Valley, J. W. *Geochem. Cosmochem. Acta* **2007**, *71*, 3887−3903.
(31) Mann, J. L.; Vocke, R. D.; Kelly, W. R. *Rapid Comm. Mass Spectrosc.* **2009**, *23* (8), 1116−1124.
(32) Walters, C. C.; Kelemen, S. R.; Kwiatek, P. J.; Pottorf, R. J.; Mankiewiez, P. J.; Curry, D. J.; Putney, K. *Org. Geochem.* **2006**, *37* (4), 408−427.
(33) Kelemen, S. R.; Walters, C. C.; Kwiatek, P. J.; Afeworki, M.; Sansone, M.; Freund, H.; Pottorf, R. J.; Machel, H. G.; Zhang, T. W.; Ellis, G. S.; Tang, Y. C.; Peters, K. E. *Org. Geochem.* **2008**, *39* (8), 1137−1143.
(34) Kelemen, S.; Siskin, M.; Gorbaty, M.; Ferrughelli, D.; Kwiatek, P.; Brown, L.; Eppig, C.; Kennedy, R. *Energy Fuels* **2007**, *21* (2), 927−940.
(35) Fitzsimons, I. C. W.; Harte, B.; Clark, R. M. *Mineral. Mag.* **2000**, *64*, 59−83.
(36) White, F. A.; Wood, G. M. *Mass Spectrometry: Applications in Science and Engineering*; John Wiley & Sons, Inc.: New York, 1986; p 773.
(37) Fahey, A. *J. Rev. Sci. Instrum.* **1998**, *69* (3), 1282−1288.
(38) Sulfur isotopes are analyzed using continuous flow isotope ratio mass spectrometry (EA-IRMS). The samples are analyzed using an elemental analyzer coupled to an isotope ratio mass spectrometer through an open split interface. The prepared sample is dropped into a 1150 °C WO_3 combustion reactor, pushed along by a helium carrier stream that has been enriched with O_2. Under these conditions, the tin capsule ignites, raising the sample temperature to 1800 °C, forming SO_2. The product gas then passes through an 850 °C quartz column packed with copper wires to reduce any SO_3 into SO_2. Any water formed during combustion is then chemically scrubbed from the helium. SO_2 is separated from CO_2 and other produced gases using purge and trap columns. After the SO_2 has been trapped on the column, the column is heated releasing the SO_2 into the open split interface. Pure reference gas (SO_2) enters the mass spectrometer at specified times to ensure proper mass calibration.
(39) Sharp, Z. *Stable Isotope Geochemistry*; Pearson Prentice Hall: Upper Saddle River, NJ, 2007; p 344.
(40) Wilk, M. B.; Gnanadesikan, R. *Biometrika* **1968**, *55* (1), 1−17.
(41) Fisher, R. A. *Ann. Eugenics* **1936**, *7*, 179−188.
(42) McLachlan, G. J. *Discriminant Analysis and Statistical Pattern Recognition*; Wiley Interscience: Hoboken, NJ, 2004; p 519.
(43) Otsu, N. *IEEE Trans. Syst. Man. Cybern.* **1979**, *SMC-9*, 62−66.
(44) Efron, B.; Tibshirani, R. *An Introduction to the Bootstrap*; CRC Press: Boca Raton, FL, 1993; Vol. *57*, p 456.
(45) Box, G. E. P.; Hunter, W. G.; Hunter, J. S. *Statistics for Experimenters: An Introduction to Design, Data Analysis, and Model Building*; John Wiley and Sons: New York, 1978; p 653.
(46) NIST/SEMATECH e-Handbook of Statistical Methods. Available via the Internet at http://www.itl.nist.gov/div898/handbook/, 2013.